

Influence of different vehicle models on the dynamic response of periodic viaducts subjected to seismic waves

Lan-Lan Chen

Department of Civil Engineering, Jiangsu University, Zhenjiang, Jiangsu, 212013, P.R. China

Received 02 September 2020; Accepted 18 September 2020

ABSTRACT

To compare the effects of different vehicle models on the dynamic response of periodic viaducts (PV) under seismic waves, a moving mass-PV model and a moving mass-spring system (MSS)-PV model under seismic waves are established by using the finite element method and Fourier transform. In order to solve the dynamic response of PV under seismic waves and MSS, the dynamic response of PV under unit series moving load component is calculated first, then the motion equation of upper mass of MSS and coupled equation of PV and the lower part of MSS are established according to Newton's second law. Solving the above equations can obtain the Fourier coefficients of the MSS-PV interaction force and the Fourier coefficients of the restoring force of the MSS spring. By using the above Fourier coefficients and the dynamic responses of PV under unit series moving load component and seismic waves, the overall dynamic response of PV under seismic waves and moving MSS can be obtained finally. The process of solving the problem of the dynamic response of PV under the moving mass and seismic waves is similar to the method mentioned above, only the MSS needs to be simplified into moving mass. The research results show that the dynamic response of the PV under seismic waves and moving mass is significantly higher than that under the seismic waves and moving MSS. Therefore, the vibration of the vehicle should be taken into consideration and to get a PV response closer to the actual situation.

Key Words: Periodic viaduct; Seismic waves; moving mass-spring system; finite element; Fourier transform

I. INTRODUCTION

As a very important structural form in the construction of high-speed railways, viaducts are often designed as periodic structures. Some viaducts are built on seismic zones. Earthquakes occurring on these seismic zones will severely damage the viaduct facilities, further resulting causing huge economic losses and casualties to human society. Therefore, it is of great engineering significance to study the vehicle-periodic viaduct (PV) coupled model under earthquake. At present, the research on the coupled vibration of vehicle-bridge under earthquake mainly focuses on seismic input mode, wheelset and viaduct interaction model, vehicle model and viaduct model. For example, Japanese scholar Matsuura^[1] established a three-dimensional vehicle model, analyzed the derailment coefficient of the vehicle on the oscillating track under seismic waves, and discussed the track deformation caused by the wheel-rail contact force and the seismic action. Miyamoto et al.^[2] simplified the vehicle model and regarded the excitation effect of the simplified vehicle model on the viaduct as an excitation to the viaduct structure. At the same time, they studied the Stability and reliability of the vehicle by fixing the vehicle and the track were together. Wu and Yang et al.^[3] used a two-dimensional vehicle-bridge model to analyze the stability of trains crossing the bridge during an earthquake, and added the influence of the track system to the model. Their study shows that the vehicle damping mechanism dissipates vibration energy, resulting in a relatively small effect of the vertical motion on the stability of vehicle on the bridge. The Japan Institute of Railway Technology^[4] studied the safety of vehicles by exciting sine waves and random excitations in the transversal direction of the vehicles traveling on the bridge, and proposed a method for vehicle safety evaluation that is applicable to both input loads. Yau^[5] decomposes the total response of vehicle suspension beams into two parts: pseudo-static response and inertial-dynamic component response. The quasi-static displacement is obtained by statically applying support motion on the suspension beam, and the inertia-dynamic component and the control equation of the mobile oscillator are converted into a set of coupled generalized equations by the Galerkin method. Treat all nonlinear coupled terms as quasi-static forces, and use Newmark method and incremental iteration method to solve the equations. Paraskeva^[6] considered the seismic response of the parallel vehicle-bridge dynamic interaction and investigated the seismic response of the vehicle-bridge interaction (VBI) system under vertical seismic excitation. He also studied the influence of traffic parameters (ie speed, number and distance between moving vehicles) and emphasized the influence of positions of vehicles during earthquakes. In his research, two main sources of dynamic excitation, which are (vertical) road conditions and (vertical) seismic ground motion, and their relative importance are pointed out.

In the study of vehicle-bridge coupled under earthquake, vehicle models have undergone the evolution from simple moving loads to half-vehicle models and full-vehicle models. This paper will establish a coupled model of vehicle-periodic viaduct (PV) under seismic waves, and study the effect of the vehicle's moving mass model and moving mass-spring system (MSS) on the dynamic response of the viaduct.

II. THE DYNAMIC RESPONSE OF PV UNDER SEISMIC WAVES AND THE VEHICLE

2.1 Mechanical model of PV and the vehicle

The viaduct studied in this paper is an infinite periodic viaduct (PV), which is composed of infinite number of identical spans. The beams between adjacent spans are connected by springs and the pier is rigidly supported on the ground. In order to facilitate the establishment of the PV calculation model in the frequency-wavenumber domain, it is assumed that the half-space soil is a homogeneous linear elastic body. In order to ensure periodicity, the geometric and material parameters of each span must be the same, and a fixed interval must be maintained. The model of PV and MSS is shown in Figure 1. MSS is composed of upper mass (M_v), lower mass (M_w), upper spring, lower spring, and damping parallel to the upper spring. The model of the PV and the moving mass is similar to that in Figure 1, just replace the MSS with the moving mass.

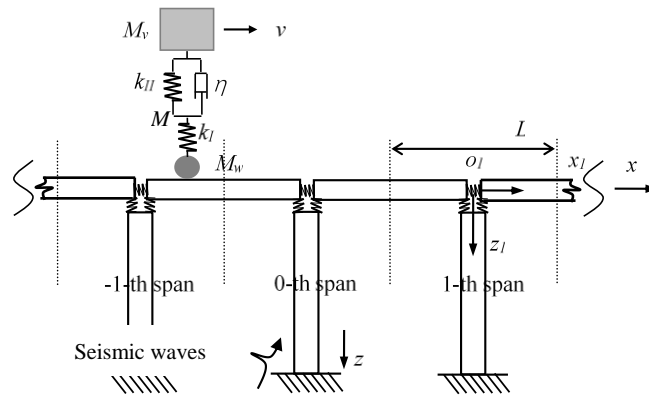


Figure.1. Mechanical model of moving MSS and PV under seismic waves.

2.2 Solving the dynamic response of PV under the action of MSS and seismic waves

This paper uses simple harmonic waves to simulate the seismic waves, the expression of the simple harmonic seismic waves is as follows

$$\Gamma(x, t) = \Gamma_a e^{i(\omega_s t - k_s x)} \quad (1)$$

where ω_s and k_s are the angular frequency and wave number of the seismic wave on the x-axis, and Γ_a represents the amplitude of the seismic waves.

When PV is subjected to the simple harmonic wave shown in formula (1), steady-state forced vibration will occur. The responses at the corresponding positions of different spans have a fixed phase difference. Use $\Phi^{(n)}$ and Φ to represent the dynamic response of the n-th and 0-th spans of the PV, then

$$\Phi^{(n)}(t) = \Phi(t) e^{i(\omega_s t - ink_s L)}, \quad \Phi(\mathbf{x}_e, t) = \Phi_a(\mathbf{x}_e) e^{i\omega_s t}, \quad \Phi^{(n)}(\mathbf{x}_e, t) = \Phi_a^{(n)}(\mathbf{x}_e) e^{i\omega_s t} \quad (2)$$

Where \mathbf{X}_e represents a point on the PV, and L represents the length of each span.

The PV dynamic response caused by the vehicle's own gravity can be solved by the method proposed in [7], so it is not considered here. The interaction force between the moving mass and PV is $\hat{f}_\alpha(\tau)$ ($\alpha = I, O$), where the subscripts I and O represent the in-plane and out-of-plane interaction forces, respectively. The interaction force between MSS and PV is $f_\alpha^{(C)}(\tau)$, and the two interaction forces are collectively called the vehicle-bridge interaction force.

The time domain response of PV to the j-th unit moving load component can be expressed as follows

$$\begin{aligned} \chi_\alpha^{(F_j)}(x, t) &= \left(\frac{1}{2\pi} \right)^2 \int_{-\infty}^{+\infty} \int_{-\infty}^{+\infty} 2\pi e^{i(k_j - k_s)\xi^{(0)}} \delta(\omega - \Omega_j - kv - \psi') \hat{h}_{\chi\alpha}(x, k, \omega) e^{i\omega t} dk d\omega \\ &= \frac{1}{2\pi v} \int_{-\infty}^{+\infty} e^{i(k_j - k_s)\xi^{(0)}} \hat{h}_{\chi\alpha}(x, k_j, \omega) e^{i\omega t} d\omega, \quad k_j = \frac{\omega - \Omega_j}{v} - \frac{\psi'}{v}. \end{aligned} \quad (3)$$

where $\chi_\alpha^{(F_j)}(x, t)$ is the time domain response of PV to the unit moving load component of the j-th order. $\hat{h}_{\chi\alpha}(x, k, \omega)$ is the frequency-wavenumber domain response of PV to the unit harmonic load $e^{i(\omega t - kx)}$ and

$\psi(\tau) = \omega_s \tau - k_s \xi$, ψ' are ψ derivatives with respect to time and $\psi' = \omega_s - k_s v$. ξ is the position coordinate of the moving mass on the x axis and $\xi = \xi^{(0)} + v\tau$, among which τ is the time, and $\xi^{(0)}$ is the position of the moving mass at the zero moment.

2.3 Method of determining the vehicle-bridge interaction force and spring force

In the above sections, methods for solving the dynamic response of PV to unit harmonic loads and harmonic seismic waves are proposed. This section will focus on how to determine the Fourier coefficient of the vehicle-bridge interaction force, and then obtain the vehicle-bridge interaction force, and use this force to determine the dynamic response of the PV caused by the force of the vehicle on the PV. The spring force is also solved in the MSS vehicle model. For the moving mass, Newton's second law can be obtained

$$-f_\alpha(t) = M a_{M\alpha}(t), \quad \alpha = I, O \quad (4)$$

where M is the mass of the moving mass; $f_\alpha(t)$ is the force acting on the PV by the moving mass; $a_{M\alpha}(t)$ is the acceleration of the moving mass.

Applying Newton's second law to MSS lower mass M_w and upper mass M_v can be obtained

$$f_\alpha^{(V)}(t) - f_\alpha^{(C)}(t) = M_w a_{w\alpha}(t), \quad \alpha = I, O \quad (5)$$

$$-f_\alpha^{(V)}(t) = M_v a_{v\alpha}(t), \quad \alpha = I, O \quad (6)$$

where M_w is mass of the lower mass of the MSS; $f_\alpha^{(V)}(t)$ is the force of the lower spring acting on the lower mass, which is called spring force in this paper; the displacement of the PV beam consists of two parts: the first part is caused by seismic waves and can be obtained by solving the finite element equation under the action of seismic waves; the second part is caused by the vehicle-bridge interaction force. Therefore, the displacement of the PV beam and the acceleration of the vehicle can be expressed as

$$v_{ba}(x, t) = v_{ba}^{(S)}(x, t) + v_{ba}^{(F)}(x, t), \quad a_{M\alpha}(t) = a_{M\alpha}^{(S)}(t) + a_{M\alpha}^{(F)}(t), \quad \alpha = I, O \quad (7)$$

where $v_{ba}^{(S)}(x, t)$ and $a_{M\alpha}^{(S)}(t)$ are the displacement of the PV beam and the acceleration of the vehicle caused by seismic waves; $v_{ba}^{(F)}(x, t)$ and $a_{M\alpha}^{(F)}(t)$ are the displacement of the beam and the acceleration of the vehicle caused by the interaction force between the vehicle and the bridge. Same as the solution method of equation (10) in the literature [7], the equation (5), (6) and (7) can be modified as

$$-\hat{f}_{ak} - M \sum_{n=-\infty}^{\infty} \hat{f}_{an} \hat{a}_{Mak}^{(F_n)} = M \hat{a}_{Mak}^{(S)}, \quad k \in (-\infty, +\infty) \quad (8)$$

$$-\hat{f}_{ak}^{(C)} - M_w \sum_{n=-\infty}^{\infty} \hat{f}_{an}^{(C)} \hat{a}_{wak}^{(F_n)} + \hat{f}_{ak}^{(V)} = M_w \hat{a}_{wak}^{(S)}, \quad k \in (-\infty, +\infty) \quad (9)$$

$$M_v \sum_{n=-\infty}^{\infty} \hat{f}_{an}^{(C)} \hat{a}_{wak}^{(F_n)} + \hat{f}_{ak}^{(V)} - M_v (\Omega_j + \psi')^2 \left[\frac{1}{k_l} + \frac{1}{k_{ll} + i\eta(\Omega_k + \psi')} \right] \hat{f}_{ak}^{(V)} = -M_v \hat{a}_{wak}^{(S)}, \quad k \in (-\infty, +\infty) \quad (10)$$

The method of solving the coupled equations (8), (9) and (10) is the same as that in the literature [7]. Finally, the acceleration Fourier coefficients are obtained by solving the equations, and the velocity Fourier coefficients are substituted into the coupled equations to obtain the Fourier coefficients. Obtain the overall response of PV under seismic waves and vehicles

$$\chi_\alpha^{(F)}(x, t) = \sum_{j=-\infty}^{\infty} \hat{f}_{\alpha j} \tilde{\chi}_\alpha^{(F_j)}(x, t), \quad \tilde{\chi}_\alpha^{(F)}(x, \omega) = \sum_{j=-\infty}^{\infty} \hat{f}_{\alpha j} \tilde{\chi}_\alpha^{(F_j)}(x, \omega) \quad (11)$$

where $\chi_\alpha^{(F)}(x, t)$ and $\tilde{\chi}_\alpha^{(F)}(x, \omega)$ refer to the total time domain and frequency domain response of PV to the moving load $F_a(\xi, \tau)$, which can represent any physical quantity of PV. $\chi_\alpha^{(F_j)}(x, t)$ and $\tilde{\chi}_\alpha^{(F_j)}(x, \omega)$ are the time domain and frequency domain response of PV to the unit moving load component of the j -th order.

III. NUMERICAL SIMULATION

This section compares the effects of moving mass and moving MSS on the dynamic response of PV numerically. The beams of each span are discretized by 120 elements, and the piers of each span are discretized by 16 elements. The number of sampling points in the frequency domain is 60001 points; and the time step of the discrete Fourier transform is equal to the time when the unit load passes through 2 beam elements; and the vehicle speed is 100m/s. The beam and pier parameters are shown in Table 1 and Table 2. The Mb of each span of the viaduct in the moving MSS model is 7.776×10^5 kg, and the mass of the upper carriage is $M_v = M_b/5$. The mass of the upper carriage is 8 times the mass (M_w) of the lower bogie. The stiffness of the upper spring and the lower spring are both 2.0×10^7 N/m, and the damping is 1.0×10^5 N*s/m. Suppose the mass of the moving mass is equal to the upper mass plus the lower mass of the moving MSS model. In addition, both vehicle models use the

same Rayleigh wave to simulate seismic waves. The results of the numerical analysis are as follows. It can be seen from Figure 2 that the change in the vehicle-bridge interaction force caused by the action of seismic waves and moving masses is greater than that caused by the action of seismic waves and MSS, and the latter changes more gently with the x -axis; in addition, the magnitude of the interaction force caused by mass is significantly higher than the magnitude of the interaction force caused by MSS.

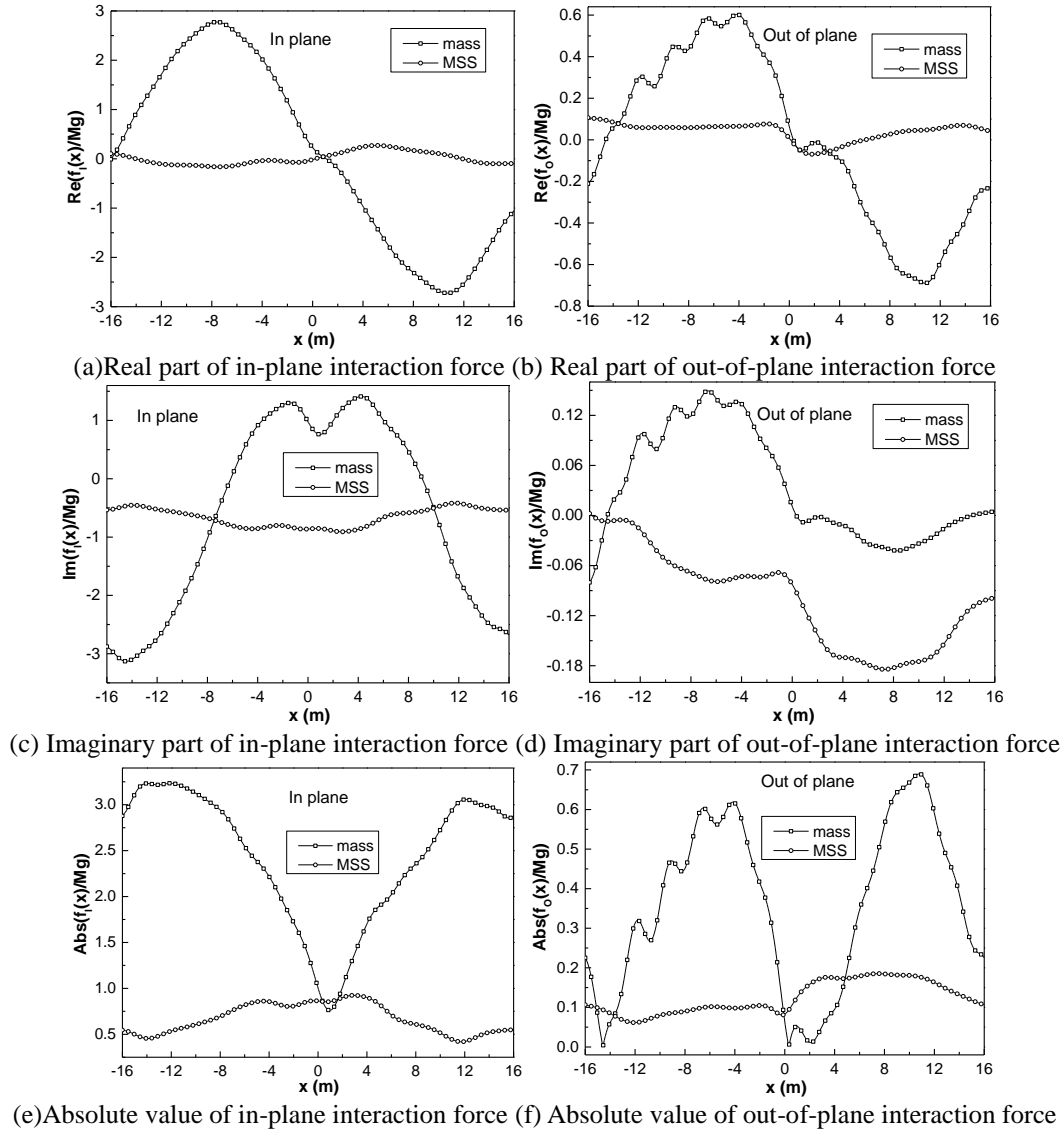


Figure.2. The vehicle-bridge interaction force under seismic waves and moving mass and under seismic waves and MSS.

Observing Figure 3, we can see that in terms of in-plane conditions, the in-plane transversal displacement of PV caused by seismic waves and moving masses is always higher than that caused by seismic waves and MSS; in terms of out-of-plane conditions, seismic waves and The PV out-of-plane transversal displacement caused by the moving mass is higher than the PV out-of-plane transversal displacement caused by seismic waves and MSS at most positions, and the amplitude of the two is similar at other positions. In addition, the change of the PV response corresponding to the moving mass model is significantly greater than the change of the PV response corresponding to the MSS model, and the latter changes very smoothly along the x -axis.

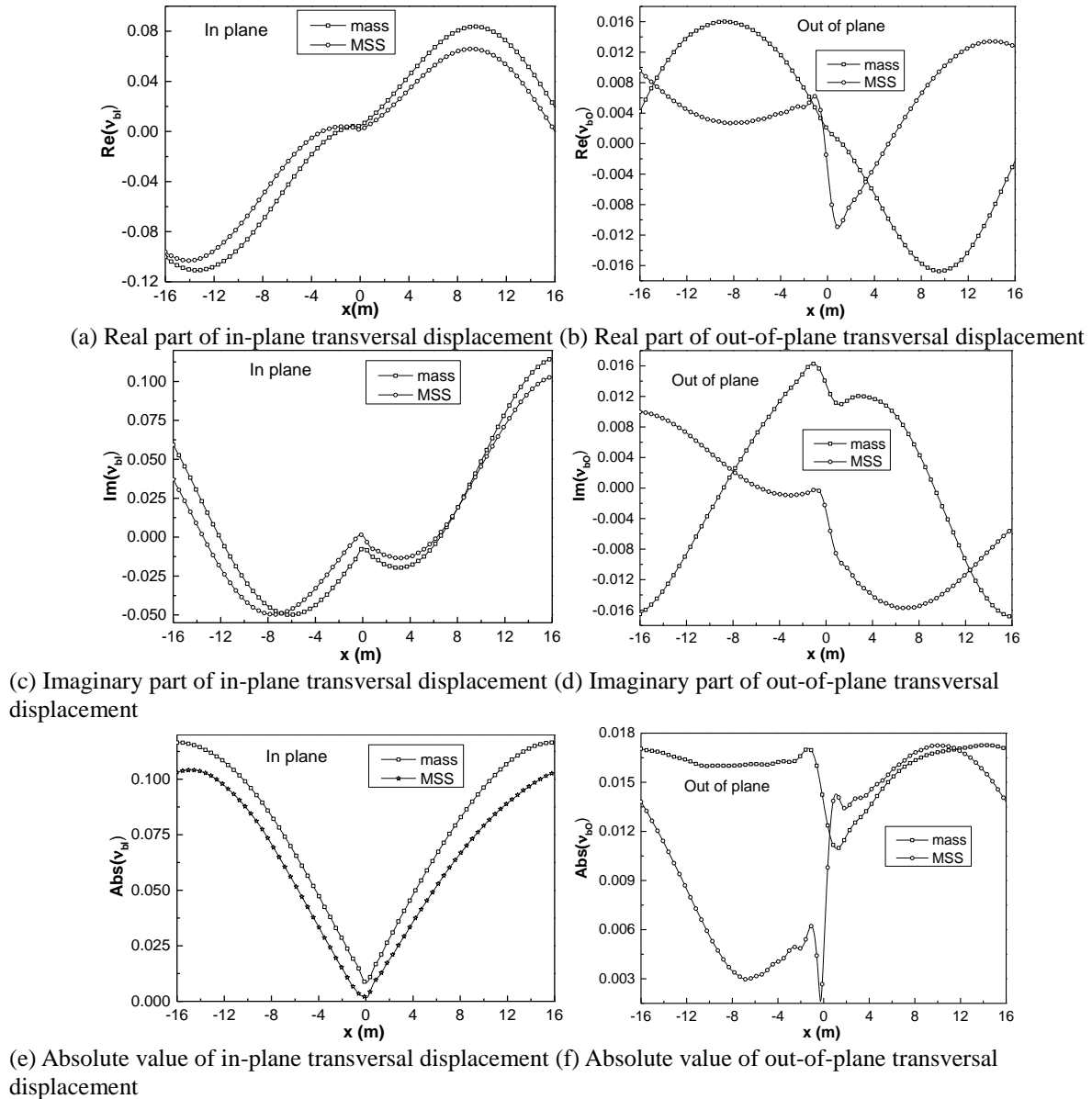


Figure.3. Transversal displacement of beam of the cell under seismic waves and moving mass and under seismic waves and MSS.

IV. CONCLUSION

This paper established a vehicle-PV coupled vibration model under seismic waves using the FEM and the FT, and simplified the vehicle into two models, which are moving mass and moving MSS. Finally compared the dynamic responses of PV caused by these two models. The numerical results show that the PV dynamic response changes caused by the moving mass are larger and the response amplitude is significantly higher than that caused by the MSS, which means that the use of moving mass to simulate a vehicle will lead to larger errors. Therefore, the vibration of the vehicle should be taken into consideration and to get a PV response closer to the actual situation.

Table.1. Material parameters of beam and pier in numerical examples

Parameter	Value	Unit
The Young's modulus of the beam and pier when $\omega \rightarrow \infty$ ($E_{b\infty}, E_{d\infty}$)	$4.0 \times 10^{10}, 4.0 \times 10^{10}$	Pa
The ratio of the Young's modulus of the beam and pier when $\omega \rightarrow 0$ to that when $\omega \rightarrow \infty$ (β_b, β_d)	0.58, 0.58	

The exponent in the Cole-Cole model for the beam and pier (α_b, α_d)	0.18, 0.18	
The characteristic relaxation time of the beam and pier (η_b, η_d)	$1.0 \times 10^{-3}, 1.0 \times 10^{-3}$	s
Poisson's ratios of the beam and pier (ν_b, ν_d)	0.2, 0.2	
Density of the beam and pier (ρ_b, ρ_d)	$2.7 \times 10^3, 2.7 \times 10^3$	kg/m ³
Length of the span of the beam (L)	32	m
The width of the cross-section of the beam (w_b)	6.0	m
The depth of the cross-section of the beam (h_b)	1.5	m
The radius of the pier (R_d)	1.5	m
The height of the pier (L_d)	12	m
The shear force coefficient of the half-space soil (μ_s)	1×10^7	Pa
Poisson's ratios of the half-space soil (ν_s)	0.4	
Density of the half-space soil (ρ_s)	2.0×10^3	kg/m ³

Table.2. The spring stiffness of beam-pier connection in numerical examples

Parameter	Value	Unit
The stiffnesses of the beam-beam spring for the in-plane deformation (k'_i, k''_i, k''_i)	$5.0 \times 10^7, 5.0 \times 10^7, 1.0 \times 10^7$	N/m, N/m N·m/rad
The stiffnesses of the left beam-pier spring for the in-plane deformation (k'_l, k''_l, k''_l)	$5.0 \times 10^8, 1.0 \times 10^7, 1.0 \times 10^7$	N/m, N/m N·m/rad
The stiffnesses of the right beam-pier spring for the in-plane deformation (k'_r, k''_r, k''_r)	$5.0 \times 10^8, 1.0 \times 10^7, 1.0 \times 10^7$	N/m, N/m N·m/rad
The stiffnesses of the beam-beam spring for the out-of-plane deformation (k'_o, k''_o, k''_o)	$5.0 \times 10^7, 5.0 \times 10^7, 1.0 \times 10^7$	N·m/rad, N/m N·m/rad
The stiffnesses of the left beam-pier spring for the out-of-plane deformation (k'_l, k''_l, k''_l)	$5.0 \times 10^8, 1.0 \times 10^7, 1.0 \times 10^7$	N·m/rad, N/m N·m/rad
The stiffnesses of the right beam-pier spring for the out-of-plane deformation (k'_r, k''_r, k''_r)	$5.0 \times 10^8, 1.0 \times 10^7, 1.0 \times 10^7$	N·m/rad, N/m N·m/rad

REFERENCE

- [1]. Matsuura A. Dynamic behavior of bridge girder for high speed railway bridge[J]. Railway Technical Research Institute Quarterly Reports, 1979, 20(02):35-42.
- [2]. Miyamoto T, Ishida H, Matsuo M. The dynamic behavior of railway vehicle during earthquake. vehicle dynamics simulation on track vibrating in transversal & vertical directions[J]. Transactions of the Japan Society of Mechanical Engineers Series C, 1998, 64(626):3928-3935.
- [3]. Wu Y S, Yang Y B, Yau J D. Three-dimensional analysis of train-rail-bridge interaction problems[J]. Vehicle System Dynamics, 2001, 36(01):1-35.
- [4]. Miyamoto T, Ishida H. Numerical analysis focusing on the running safety of an improved bogie during seismic vibration[J]. Quarter Reporter of RTRI, 2008, 49(03):173-177.
- [5]. Yau J D. Response of a train moving on multi-span railway bridges undergoing ground settlement[J]. Engineering Structures, 2009, 31(09):2115-2122.
- [6]. Paraskeva T S, et al. Dynamic vehicle-bridge interaction under simultaneous vertical earthquake excitation[J]. Bulletin of Earthquake Engineering, 2016, 15(1).
- [7]. Lu J F, Feng Q S, Jin D D. A dynamic model for the response of a periodic viaduct under a moving mass [J]. Elsevier Masson SAS, 2018, 73(suppl):394-406.

Lan-Lan Chen. "Influence of different vehicle models on the dynamic response of periodic viaducts subjected to seismic waves." *IOSR Journal of Engineering (IOSRJEN)*, 10(9), 2020, pp. 45-50.